JOURNAL OF CATALYSIS **163,** 262–270 (1996)
ARTICLE NO. 0327

Acid Catalysts Based on Cu/Ru Alumina: Conversion of Butyraldehyde to Dibutyl Ether

Susan Jansen,* Michael Palmieri,* Maria Gomez,* and Steve Lawrence†

*Department of Chemistry, Temple University, Philadelphia, Pennsylvania 19122; and †Department of Chemistry, Saginaw Valley State University, University Center, Michigan 48710

Received July 6, 1995; revised May 15, 1996; accepted May 24, 1996

A system made by combining two nonalloying metals, ruthenuim and copper, using alumina as the oxide support was studied. This bimetallic supported catalyst has been used mainly in hydrogenolysis, dehydrogenation, and oxidation reactions of hydrocarbons. The preparation of such materials has been proposed to effect the selectivity and activity of a highly active metal by inclusion of a second less active metal. The samples were characterized by electron paramagnetic resonance spectrometry (EPR), X-ray diffraction (XRD), surface area, and surface acidities. The techniques EPR and XRD are ideal for studying the electronic and structural changes of the samples at different temperatures and concentrations. The primary reaction involved in this study was the hydrogenation of an aldehyde to the corresponding alcohol. A secondary reaction occurred as well. The acid catalyzed, substitution or bimolecular dehydration of the alcohol to the dibutyl ether was observed under certain catalytic conditions. These catalysts appeared to act as acid/base. Therefore this reaction to produce the ether is of special importance. A correlation between the electronic, structural and catalytic properties has been made to understand molecular processes' role in catalytic phenomena.

INTRODUCTION

In the past 20 years there have been multiple reports on mixed metal catalysts (1–5). The general motivation for the preparation and study of such materials has been to affect the selectivity of a highly active metal by inclusion of a second less active metal. The primary metal is supposed to be the "active" component while the secondary metal is chosen to induce a pronounced selectivity in the catalytic reaction. Furthermore, the metallic components were selected based on certain electronic and packing characteristics including metals capable of forming alloys in the metallic state such as nickel and copper, copper and gold, and ruthenium and copper. Nickel and copper and copper and gold are known to form alloys in the bulk while it has been determined that copper can grow pseudomorphically atop the (0001) surface of ruthenium with very little tensile strain. Copper and ruthenium, however, show no significant propensity to alloy (6). Catalytic applications require that these materials be supported on oxide substrates, usually silica or alumina. As was anticipated, the catalytic properties of the mixed metal systems varied widely depending on the preparation, support characteristics, and catalytic application; i.e., varying effects on activity and selectivity were observed for oxidation and reduction.

In this study we focused on electronic features in $Cu/Ru/Al_2O_3$ systems that define the catalytic properties of a fairly simple bimetallic catalyst. The metals were chosen for several reasons. (i) Copper aluminates, which adopt the spinel structure, are known to form in preparation of ceramic materials (7). The inclusion of a secondary metal may affect the formation of the stable spinel structure and the metal oxide surface state. (ii) Formation of ruthenium oxides or related integrated ruthenium-copper oxides are expected to exhibit modified electronic properties. (iii) The structural data obtained will be of utility for the assessment of catalytic properties of mixed metal systems. To date, attempts at correlation of the catalytic or electronic properties with the structural or electronic phases produced during preparation or surface catalytic species have proven difficult. This is in part because direct characterization of the structural phases has been limited. Here, a variety of structural, electronic and chemical tools were applied to assess the surface and bulk properties of the copper-ruthenium system.

Catalytically, ruthenium dioxide is primarily uased for oxidation of hydrocarbons and for hydrogenation and dehydrogenation of alkanes (8). Copper oxide is primarily used for oxidation of hydrocarbons, dehydration, dehydrogenation of alcohols, and reduction of aldehydes (9). The bimetallic system is typically used for hydrogenolysis, dehydrogenation, and oxidation of hydrocarbons (10). This work will provide an extensive characterization of the catalytic properties of a copper-ruthenium system supported on alumina. The hydrogenation reaction of butyraldehyde was used to study the chemistry of the $Ru–Cu/Al_2O_3$ catalysts. The active species in this reaction was expected to be the cupric sites from copper oxide which is primarily used for the reduction of aldehydes to alcohols and the

0021-9517/96 $18.00

oxidation of alcohols to aldehydes. The oxygen atom of the RCOH and ROH is understood to be the site of attachment for the reactant at a copper/CuO site on the surface. The catalytic reduction of the aldehyde to its corresponding alcohol, typically proceeds with the adsorption of the aldehyde onto the catalyst and then dissociative adsorption of H_2 and H addition across the C=O bond. With addition of the hydrogen across the C=O bond the aldehyde is reduced/hydrogenated to the corresponding alcohol.

The alcohol may further react to produce certain ethers. It is well known that the synthesis of symmetrical dialkyl ethers (dibutyl ether) can occur by bimolecular dehydration from simple unhindered primary alcohols (1-butanol). Under acidic dehydration conditions two reactions compete: elimination to give an alkene and substitution to give an ether. Substitution to produce the ether is a bimolecular dehydration and the elimination reaction to form the alkene is a unimolecular hydration (11).

In general, the later transition metals like ruthenium (RuO_2) and copper (CuO) on oxide supports have not been thought of as having sufficient acidic properties to affect ether synthesis. The earlier transition metal oxides such as tungsten (WO_3) and molybdenum (MoO_3) on an oxide support (TiO_2) have been shown to have greater surface acidities than the support and have been used in many reactions such as oxidation of methanol to formaldehyde and hydration of propylene (12–14). Not surprisingly Ru/Al_2O_3 and Cu/Al_2O_3 systems have rarely been used as acid catalysts and have been used mainly for hydrogenation, dehydrogenation of alkanes, oxidation of alcohols, and reduction of aldehydes. Even though there are few papers discussing the catalysis of the $Ru–Cu/Al_2O_3$ mixed metal system, the catalytic applications usually parallel the individual uses of RuO_2 and CuO on alumina. In this work it will be shown that ruthenium and copper supported on an oxide substrate has measurable surface acidity and can be used as an acid catalyst, as in the formation of dibutyl ether as well as other dialkyl ethers. Their potential as bifunctional or multifunctional catalysts will be discussed in this paper.

Due to environmental concerns and new stringent environmental laws, there is a shift toward developing new "cleaner" burning fuels. Ethers, such as methyl tertiary butyl ether (MTBE), ethyl tertiary butyl ether (ETBE), and tertiary amyl ether (TAME) have been shown to be cleaner burning fuels but MTBE is the most widely used of the ethers. ETBE and TAME have not found wide applications due to the relative high cost of ethanol compared to methanol and the limited availability of iso-pentene relative to iso-butene (15) as they offer volatility advantages to MTBE. Developing better and more cost effective processes for making these higher ethers is important. Catalysis will play a significant role in developing new routes for these more environmentally safe fuels. Therefore new inexpensive catalytic routes to alternative ether components other than MTBE would be advantageous particularly if crude olefinic refinery streams could be used as feedstock (16–18).

EXPERIMENTAL

I. Preparation of Materials

The materials were prepared by the incipient wetness method (19), in which two different procedures were employed. These are termed (i) "simultaneous" and (ii) "stepwise" depositions: (i) In simultaneous deposition the impregnating solutions containing the two metal salts [$CuNO_3 \cdot 6H_2O$ (0.0393 *M*) and $RuCl_3 \cdot xH_2O$ (0.0247 *M*) were added to the alumina simultaneously. The two metal salts were purchased from Aldrich Chemical Company and the alumina support (150 m^2/g, 80–200 mesh) was purchased from Fisher Chem Alert. (ii) The step-wise deposition method divides the addition of the impregnating solutions into two steps. First, one metal solution was added to the alumina, dried (100°C for 10 h), and then calcined (300°C for 12 h). The second metal solution was then added and the final heat treatments were performed. These catalysts all contained 1% rethenium by weight with varying amounts of copper (0.15 to 1.1 wt%).

The actual metal content/loading was determined by atomic absorption (AA). The AA measurements were performed on a BUCK Scientific (Model 200A) instrument. The theoretical and actual amounts of metal content are reported in Table 1.

II. Electron Paramagnetic Resonance (EPR)

EPR measurements were performed on a Bruker ER-200D spectrometer, fitted with an ER035 gaussmeter to provide accurate magnetic field measurement to 0.001 G/1000 G. For variable temperature measurements, temperature control was maintained by a VT-4114 unit

TABLE 1

Materials, Percentage Loadings, Surface Areas and Hammett Acidities

Catalyst	Ru (wt%)	Cu (wt%)	Mole Cu–Ru	Surface areas (m^2/g)	H_0
Cu/Al_2O_3	0.00	14.6(14.55)	—	222	~ NA
Cu/Al_2O_3	0.00	1.0(0.97)	—	212	~ +2
Ru/Al_2O_3	1.0(0.99)	0.00	—	197	~ +1
$Ru–Al_2O_3–Cu$	1.0(1.01)	0.15(0.16)	0.25	204	~ +2
$Ru–Al_2O_3–Cu$	1.0(1.05)	1.1(1.13)	1.50	209	~ +2
$Ru–Cu/Al_2O_3$	1.0(1.06)	0.15(0.14)	0.25	204	~ +2
$Ru–Cu/Al_2O_3$	1.0(1.03)	1.1(1.14)	1.50	209	~ +2
Al_2O_3[a]	0.00	0.00	0.00	152	~ +1

Note. The numbers in the parentheses are the actual weight percents determined by AA.

[a] Support.

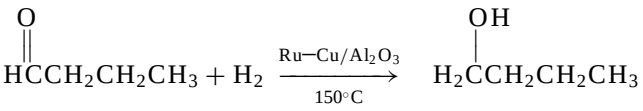

SCHEME I. Reduction/hydrogenation of aldehyde to alcohol.

which maintains temperature within 0.5°C. A series of EPR measurements wwere made on materials in which the overall loading was relatively low, 1–3% by weight. For these samples, the theoretical coverage limits were less than one-tenth of a monolayer and as such, these materials provided the potential for analysis of isolated metal-oxide interaction. The potential for aggregation can also be addressed, as any cooperative metal-metal/oxide interaction will appear rather pronounced in the EPR characterization at such low loadings and coverages. A complementary study at high loading, 1/2 and full monolayer, i.e., 15–35% by weight was also undertaken to determine the structural limits affecting catalytic and electronic properties.

III. Catalyst Characterization

The calcined materials were characterized by XRD. XRD measurements were performed on samples which ranged from 1 to 2% in copper and ruthenium. Surface area measurements for the highly loaded/low dispersion and low loaded/high dispersion calcined materials were determined using a liqud N_2 BET adsorption apparatus. Acidities were assessed by surface state titration. The surface acidity of these samples was evaluated using the *n*-butylamine titration method established by Tanabe (20–24). The total acidity is related to the number of sites having acid strengths with $H_0 \leq +2.0$. The composition, surface areas and relative Hammett acidities are reported in Table 1. Infrared spectra recorded during temperature-programmed decomposition (TPD) measurements of ammonia, monomethylamine (MMA), dimethylamine (DMA), and trimethylamine (TMA) have shown that alumina and alumina supported metal catalysts contain Lewis—as well as Brønsted—acid sites (25–28).

IV. Catalysis: Analysis of Reaction Mixture

In order to understand the interaction of copper (copper oxide) and ruthenium (ruthenium dioxide) on the support, a study was performed by choosing a reaction that was suitable for copper (CuO) states. This enabled us to study the effects that ruthenium would have on copper. The reaction of interest was the hydrogenation (reduction) of an aldehyde (butyraldehyde) to its corresponding alcohol (1-butanol) with the possible formation of the subsequent ether (dibutyl ether). These two reactions are shown in Schemes I and II. These catalysts were studied by a gas-solid reaction which was carried out under continuous-flow conditions in a glass tubular reactor (29). The reactor tube was mounted in a tube furnace and the feed stream was 100% hydrogen. Since the products were in the gas phase, GC was the method employed to study the reaction. The column used was a 0.10% SP-1000, 80/100 carbopack, and $6' \times 1/8''$ in size. The reaction conditions used for the reduction of butyraldehyde to 1-butanol was a temperature of 150°C, a hydrogen flow of 10ml/min, and 160 mg of catalyst.

RESULTS AND DISCUSSION

XRD

The structural characterization of the calcined catalysts was performed by XRD on the highly loaded and low loaded materials. The highly loaded pure copper on alumina showed crystalline CuO, Al_2O_3, and AlOOH peaks, whereas the low loaded pure copper on alumina showed Al_2O_3 and AlOOH peaks, only. It has been determined from the XRD that the major components of the alumina are the Al_2O_3 and AlOOH peaks. Using a peak finding program (JCPDS-ICDD), it was established that these peaks had an 85% correlation to the gamma phase. In the mixed metal catalysts the dominant species present in the XRD was RuO_2. CuO was not present in the X-ray diffraction spectra because it was either in a non crystalline form or present primarily at the surface. Figures. 1a and 1b show the XRD spectra.

As stated earlier, copper was chosen because it forms copper aluminates which adopt the spinel structure. The spinel structure consists of a close-packed lattice of oxide ions with one-third of the metal ions in tetrahedral sites and two-thirds of the metal ions in octahedral sites. In a "normal" spinel, the M (+2) ions occupy tetrahedral sites and the M (+3) ions occupy the octahedral sites. In an "inverse" spinel, part of the M (+3) ions exchange positions with the M (+2) ions, therefore, some of the M (+2) ions are in octahedral sites (30). Copper aluminate (Cu/Al_2O_3) is a partially inverse cubic spinel (31). The spinel structure is shown in Fig. 2. It has been shown that under certain preparation conditions copper supported on high surface area alumina forms crystalline aluminates, whereas at high level of metal on a lower surface area support, CuO was predominant (bulk material). This aluminate phase can be detected even on material calcined as low as 300°C (7, 32). In this

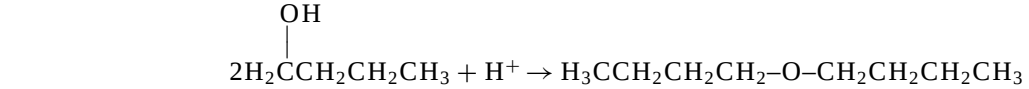

SCHEME II. Bimolecular dehydration of alcohol to dialkyl ether.

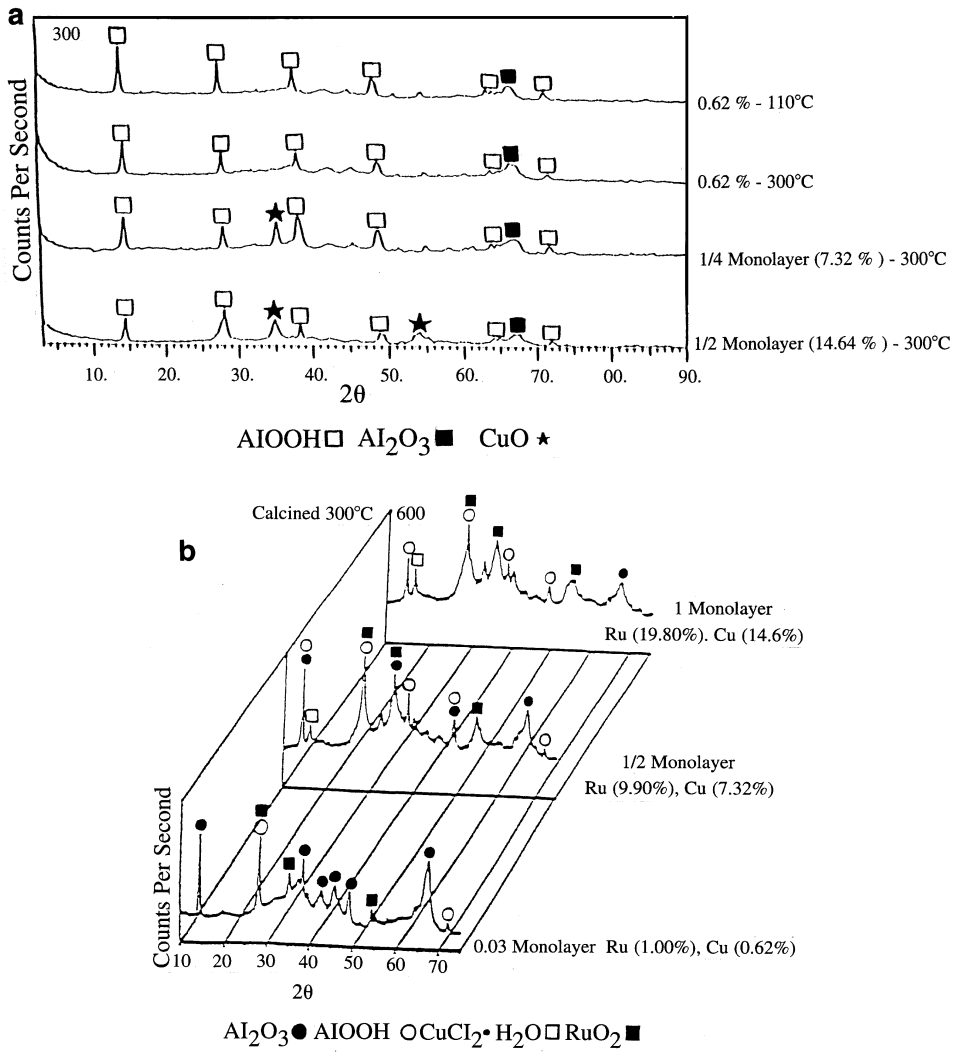

FIG. 1. (a) XRD of highly loaded and low loaded Cu/Al_2O_3. (b) XRD of highly loaded and low loaded $Ru–Cu/Al_2O_3$.

work, a moderately high surface area alumina (150 m^2/g) was used and by XRD, the spinel structure copper aluminates ($CuAl_2O_4$) were detected at a calcination temperature of 500°C. The XRD is shown in Fig. 3. Spinel formation provides a possible mechanism for Cu/Ru aggregation on alumina.

EPR

In copper(II) oxide, copper II has a d (9) electron configuration ($S = 1/2$, $I = 3/2$) and is usually present in a tetragonally distorted octahedral coordination. In this work "CuO" was the species being analyzed but it is "defect" states that give rise to the EPR signal. When copper is loaded and calcined on alumina copper oxides are formed. If significant CuO domains form, the copper centers are antiferromagnetically coupled to other copper centers and therefore are EPR silent (33, 34). The defect states are the copper centers which are observable in the EPR. This maybe due to isolation of species or "interference" from electronic factors contributed by ruthenium. Similarly, copper aluminates ($CuAl_2O_4$) are EPR silent (35). Since the only EPR signal observed for our catalysts is from a tetragonally distorted octahedral coordination, this suggests that some of the copper(II) ions are occupying the octahedral sites of the spinel. Due to these "defect" features, an EPR signal can be detected at room temperature. It has been shown in other work that the concentration of these "defect" states are proportional to the surface area (36).

There is an inverse correlation between the amount of copper loaded and the spin concentration of copper (paramagnetic species); i.e., the more copper present on alumina the lower the spin concentration (33, 34, 37). This is due to the increasing formation of CuO domains. Therefore, the highly loaded/low dispersion materials have fewer spin active species than the low loaded/high dispersion materials.

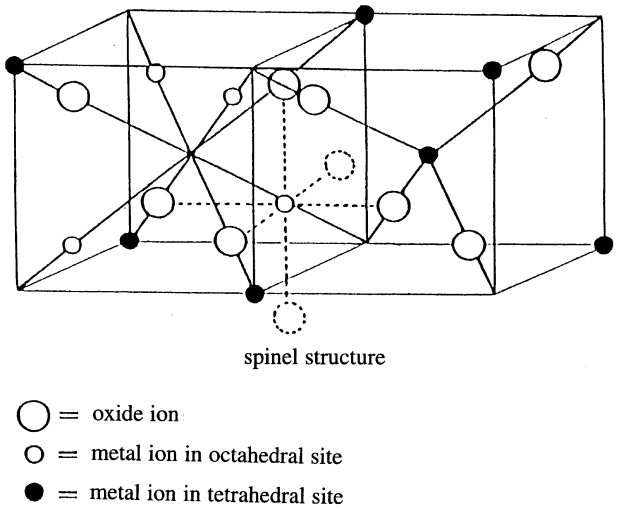

FIG. 2. Spinel structure.

The EPR spectra for the "differently" prepared catalysts, i.e., simultaneous, stepwise depositions and high and low loaded, are shown in Fig. 4.

The EPR signal for the copper species is nearly axial, where $g_{xx} = g_{yy} \neq g_{zz}$. The g and hyperfine coupling tensors can be studied and information as to coordination effects can be extracted from qualitative molecular orbital theory (38). Because the g factor is extremely sensitive to change in the chemical environment, information about the electronic environment for the copper environment as a function of preparation can be studied. Since the signal is anisotropic, $g_{\|}(g_{zz})$, $g_{\perp}(g_{xx}, g_{yy})$ and $A_{\|}$ (hyperfine coupling) can be obtained through simulation (39). These features can give insight on how the chemical environment is changing for the

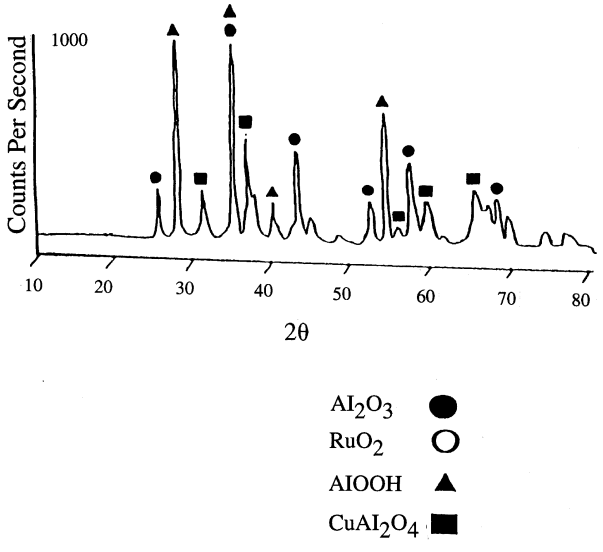

FIG. 3. XRD of the $CuAl_2O_4$ (1 wt%).

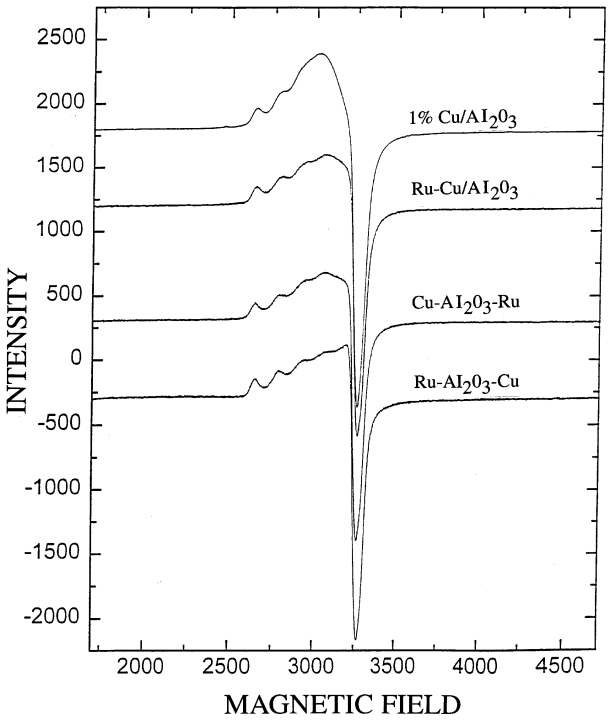

FIG. 4. The EPR spectra of the differently prepared catalysts.

copper oxide. The theory of Maki and McGarvey for EPR relates the molecular states of the cupric ion to $g_{\|}$ and $g_{\perp}$ of copper(II) complexes (38). This information can also be used to calculate the delocalization of the unpaired electron and the σ bond density, see Eqs. [1] and [2]:

$$g_{\|} = g_e - 8\lambda_0\alpha\beta_1/\Delta_{xy}\left[\alpha\beta_1 - 1/2\alpha'\left(1-\beta_1^2\right)^{1/2}T(n)\right] \quad [1]$$

$$g_{\perp} = g_e - 2\lambda_0\alpha\beta/\Delta_{xz,yz}[\alpha\beta - 1/(2)^{1/2}\alpha'(1-\beta^2)^{1/2}T(n)]. \quad [2]$$

Here α^2 is related to the delocalization of the unpaired electron, $1-\alpha^2$ is the σ bond strength between the central atom and the ligands, and α is the molecular orbital coefficient for the in plane σ bonding of the copper $(dx^2 - y^2)$ orbital. The $dx^2 - y^2$ is the orbital where the unpaired electron "resides" in a tetragonal distorted octahedral or in a square planar complex and the ΔE is approximately 15,000 cm^{-1} (40). These parameters can be calculated from (41)

$$\alpha^2 = A_{\|}/P + (g_{\|} - 2) + (3/7)(g_{\perp} - 2) + 0.04. \quad [3]$$

The EPR parameters used in the above equation were calculated using the EPR simulation program by Neese and Nilges (39). Table 2 shows a list of the EPR features for the "differently" prepared catalysts.

The EPR data suggest that there was a sizeable shift in $g_{\perp}$ for the dominant magnetic species. Further evaluation in terms of the σ bond strength and the molecular orbital

TABLE 2

EPR Features

Catalyst	$g_{\parallel}{}^a$	$g_{\perp}{}^a$	$A_{\parallel}$ (cm^{-1})	α^2	$1-\alpha^2$	α
14.6% Cu/Al_2O_3	2.3504	2.0800	0.0153	0.85	0.15	0.92
1% Cu/Al_2O_3	2.3504	2.0800	0.0153	0.85	0.15	0.92
$Cu–Al_2O_3–Ru$	2.3500	2.0750	0.0153	0.85	0.15	0.92
$Ru–Al_2O_3–Cu$	2.3504	2.0650	0.0153	0.84	0.16	0.91
$Ru–Cu/Al_2O_3$	2.3500	2.0750	0.0153	0.85	0.15	0.92
Spectral subtraction	2.3500	2.0750	0.0040	0.53	0.47	0.73

[a] These values are constant within each catalyst series/do not change with %Cu.

coefficient showed that for the dominant magnetic species there were no significant differences between the highly loaded, low loaded, and mixed metal catalysts. Evaluation of the π bonding, which is related to $g_{\perp}$ showed there was approximately a 10% change in the π bonding character between the different catalysts. This EPR data showed that the majority of the electron density was localized on the copper.

The dominant magnetic species for each catalyst seems to be similar; however, the spectra envelope for the $Ru–Al_2O_3–Cu$ showed one distinct difference when compared to the other spectra. Consequently, a spectral subtraction was performed between the $Ru–Al_2O_3–Cu$ and the $Cu–Al_2O_3–Ru$ catalysts. The catalyst in which the copper was deposited last, $Ru–Al_2O_3–Cu$, was more catalytically active than the other materials. When the ruthenium was deposited last the catalyst was relatively inactive. The results of the subtraction are shown in Fig. 5. The spectrum remaining after subtraction gives insight on the catalytically active species. This subtraction revealed that the magnetic state was more highly delocalized with the spin density being distributed over the copper(II) oxide. The loss of resolvable hyperfine suggests a more mobile electron species. This is shown in Table 2.

Catalysis

The first catalyst studied was the standard high coverage (14.6 wt%) Cu/Al_2O_3 which converted about 86.4 mole% of the butyraldehyde, giving butanol as 99% of the total products. The low loaded pure 1 wt% Cu/Al_2O_3 was studied and showed significant activity. The total conversion to product was 22 mole% with a significant selectivity toward 1-butanol. The ratio of 1-butanol to dibutyl ether (minor product) was 4.4:1, where dibutyl ether was 18% of the products. The 1% by wt Ru/Al_2O_3 was studied and showed no measurable activity. Of significant importance is that even though the 1% pure copper catalyst had 14.6 times less metal content than the highly loaded sample, the total conversion was only 4 times smaller. If the conversion was based solely on the metal content defining the metal sites, the conversion should be significantly less; however, this was not the case.

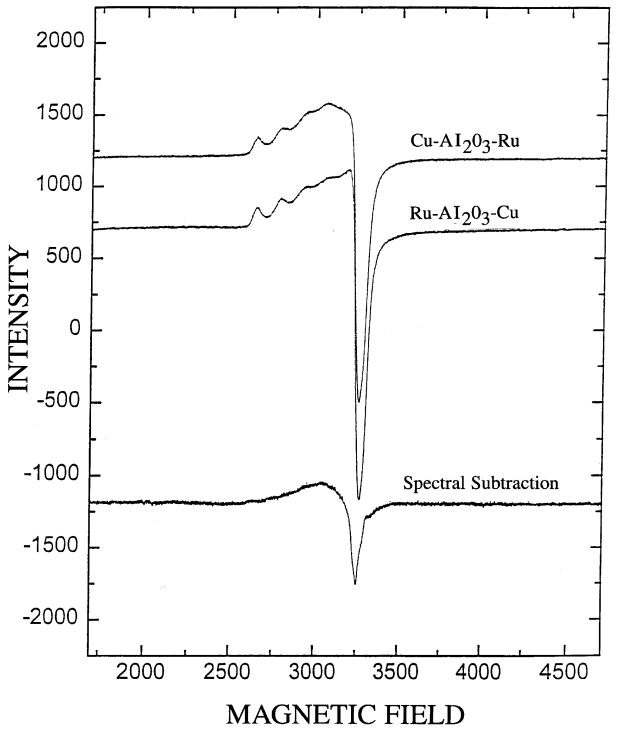

FIG. 5. The EPR spectral subtraction.

For the mixed metal catalysts of $Ru–Cu/Al_2O_3$, $Ru–Al_2O_3–Cu$, and $Cu–Al_2O_3–Ru$, the addition of ruthenium changed both the activity and the selectivity of the reduction of butyraldehyde. In addition the preparation method of these materials played a critical role in defining the activity and selectivity of the $Cu–Ru/Al_2O_3$ catalysts. In the catalysts where ruthenium was added last in the deposition order ($Cu–Al_2O_3–Ru$), the catalytic activity was lost. This is probably due to a simple site blockage by the ruthenium, since the butyraldehyde cannot adsorb onto the catalyst surface, where the adsorption sites are "masked" by ruthenium. This begs the question as to aggregation. At this loading less than 1/10th of the surface is covered. Site blockage may occur if the copper serves as a "nucleation" site for the secondary metal. Since copper appears to be the adsorption site of the reactant species, coordination with ruthenium would block the active site. Other work supports this idea (37).

Furthermore, it has also been determined that ruthenium IV (RuO_2) is reduced to ruthenium(0), during many catalytic processes, when the temperature approaches or exceeds 150°C. This is due to the decomposition of the organic material (reactant), which deposits carbon onto the surface, causing reduction of the ruthenium. When the ruthenium is in its reduced form (Ru^0) the activity of the catalyst is lost (37). In the butyraldehyde reaction the temperature of the catalytic reaction was at 150°C, so some of the reactant

may have decomposed and deposited on the catalyst, causing the ruthenium to be reduced. Evidence of this reduction was seen in the XRD spectra of the used catalyst (37). This is another process implicated in the loss in activity for the $Cu–Al_2O_3–Ru$ systems.

When the reverse deposition order is used, where copper is deposited last ($Ru–Al_2O_3–Cu$) in the preparation, the catalyst showed significant activity relative to the pure Cu/Al_2O_3 material. The total conversion to product ranged from 5 to 15 mole% depending on the relative mole ratio of copper to ruthenium. The selectivity was changed relative to the pure copper catalyst; here the ratio of 1-butanol to dibutyl ether was 3:1 and the dibutyl ether was 25% of the product formation. In the simultaneous deposition catalysts ($Cu–Ru/Al_2O_3$) the activity was reasonable, where the total conversion of product ranged from 4 to 14 mole% depending on the mole ratio of copper to ruthenium. Here the selectivity was significantly different than any of the other catalysts, the ratio of 1-butanol to dibutyl ether was 1:1 and the dibutyl ether was now 50% of the product formation. These results are summarized in Table 3.

Always of interest is the lifetime or surface stability of these systems. The lifetime of the pure Cu/Al_2O_3 catalyst is extended when ruthenium is added to the material. The catalytic activity of the 1% by wt Cu/Al_2O_3 decreased by 50% after 95 min, and after 2 h the activity decreases to 25%, where it remained constant for days. Whereas the activity of the mixed 1.5 mole ratio $Ru–Cu/Al_2O_3$ catalysts remained constant over the same period of time as the pure copper catalyst. Initially the pure copper catalyst has a higher mole percent conversion than the mixed metal catalyst, but this occurs only in the first hour. After 2 h and for the next 20 h the mixed metal catalyst was approximately 260% more effective relative to the low loaded pure copper catalyst. In addition the selectivity of the mixed metal material toward the ether product was approximately 35% more favorable than the pure copper sample. Table 4 shows the relative activity of the catalysts over 4–5 h: 1 wt% Cu/Al_2O_3 vs 1.5 mole ratio $Ru–Cu/Al_2O_3$.

TABLE 4

Relative Activity of Copper Catalyst vs Mixed Metal Catalyst

Time (min)	1 wt% Cu/Al_2O_3 (mole%)	1.5 mole ratio $Ru–Al_2O_3–Cu$ (mole%)	$Ru–Cu/Al_2O_3/Cu/Al_2O_3 \times 100$[a]
60	21.6	14.0	65%
95	10.8	14.0	130%
120[b]	5.4	14.0	260%

[a] Ratio shows the effectiveness of the mixed metal to the pure catalyst over time.

[b] The 120 min point is cosntant for the two catalysts up to and including 20 h (1200 min).

Reaction Chemistry and Proposed Mechanisms

For this catalytic reaction to be useful there must be good adsorption of the butyraldehyde onto the catalyst. In order to produce dibutyl ether, two conditions must be present. (i) 1-butanol must be present at the surface of the catalyst and (ii) the surface of the catalyst must be acidic. Table 5 shows the Hammett acidities and production of dibutyl ether.

The primary reaction is the reduction/hydrogenation of the butyraldehyde to butanol, where hydrogen dissociates across the double bond of the carbonyl group. The secondary reaction can be the bimolecular dehydration of an unhindered primary alcohol (1-butanol) to the dialkyl ether. Under acidic dehydration conditions, two reactions can compete: substitution to give the ether (bimolecular) and elimination (unimolecular) to give the alkene.

In Table 5 it is shown that the alumina support and the ruthenium on the alumina support have similar acidities, suggesting that the ruthenium had no significant effect on the acidity of the support. When the copper was added to the alumina and to the ruthenium on alumina the acidity was decreased by a factor of 10 for the low loaded catalysts and negligible (or effectively zero) for the highly loaded copper catalyst. Pure CuO is known to be considerably basic

TABLE 3

Initial Catalytic Activity and Selectivity

Catalyst	Ru (wt%)	Cu (wt%)	μmoles/ $m^2 \cdot min$	Mol%/ wt%[a]	Mol%[b]	%Butanol[c]	%Ether[c]
Cu/Al_2O_3	—	14.6	4.05×10^{-2}	5.92	86.4	99	<1%
Cu/Al_2O_3		1.0	1.03×10^{-2}	21.6	21.6	82	18
$Ru–Al_2O_3–Cu$	1.0	0.15	1.03×10^{-3}	4.7	5.4	75	25
$Ru–Al_2O_3–Cu$	1.0	1.1	6.94×10^{-3}	6.6	14.0	75	25
$Ru–Cu/Al_2O_3$	1.0	0.15	8.82×10^{-4}	4.2	4.8	50	50
$Ru–Cu/Al_2O_3$	1.0	1.1	6.84×10^{-3}	6.5	13.7	48	52

[a] Percentage by weight of total metal.

[b] Mole percentage of total product.

[c] Percentage distribution of products.

(42). This suggests that the copper oxide contributes basic sites upon formation on the alumina support. Also, it is important to note that the selectivity toward the ether was increased when ruthenium was present in the catalysts. This is probably due to the ability of ruthenium to transfer protons and increase the mobility of the hydrogen species. It has been shown that ruthenium chemisorbs hydrogen rather easily in both homogeneous and heterogeneous reactions. With the addition of copper the amount of chemisorbed hydrogen decreases (43). These mixed metal catalysts seem to be acting as multifunctional catalysts where the alumina surface may be the source of the protons (acid). The basic copper oxide functions as a Lewis base in the adsorption mechanism and is the site of attachment for the aldehyde. Ruthenium sites are implicated in the hydrogen processing.

Our proposed mechanism suggests that the aldehyde must be adsorbed onto the surface of the catalyst at the cupric site of the copper oxide islands. Once the aldehyde is bound to the surface of the catalyst, it is reduced to its corresponding alcohol. Then a secondary reaction, initiated by acidic protons distributed over the exposed alumina, occurs. This promotes the formation of the dibutyl ether. The present mechanism suggests that some of the alcohol, while present at the surface, is protonated (H^+). The H^+ which protonates the alcohol is the proton associated with the support (AlOOH). The alcohol molecules present at the surface of the catalyst which have not been protonated may act as the nucleophiles, in particular, the -OH group. The alcohol attacks the protonated alcohol forming the dialkyl ether through a substitution, bimolecular dehydration. The smaller alcohols such as methanol and ethanol are known to deprotonate when adsorbed onto CuO (acting as a Brønsted base) but the proton associated with butanol is less acidic (44), so the possibility of deprotonation is less likely to occur. A schematic drawing of the proposed mechanisms is shown in Fig. 6.

The catalytic results showed that only two products were formed, 1-butanol and the dibutyl ether. These catalysts were moderately acidic as shown by the Hammett titration,

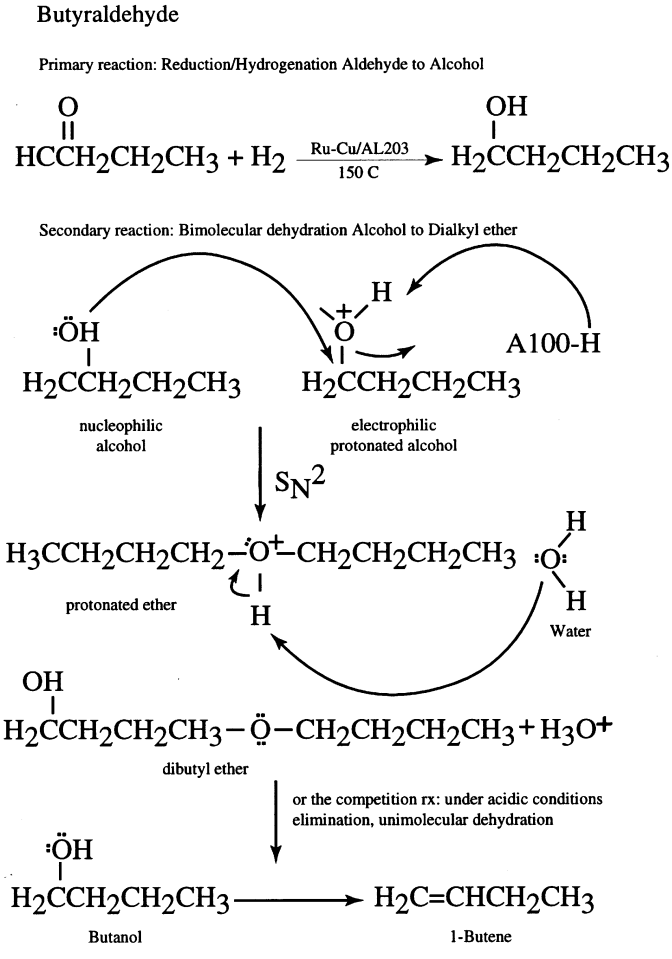

FIG. 6. Schematic of the proposed mechanisms.

so there was the possibility of the elimination, unimolecular dehydration reaction occurring to produce the alkene. The alkene was not detected; therefore, the secondary reaction is likely restricted to the bimolecular dehydration.

TABLE 5

Relationship between the Hammett Acidities and Dibutyl Ether

Catalyst	Hammett acidities	% Dibutyl ether[a]
Al_2O_3	~+1	—
Ru/Al_2O_3	~+1	—
$Cu–Al_2O_3–Ru$	~+2	—
Cu/Al_2O_3[b]	~NA	—
Cu/Al_2O_3	~+2	18
$Ru–Al_2O_3–Cu$	~+2	25
$Ru–Cu/Al_2O_3$	~+2	52

[a] Percentage of total products.
[b] Highly loaded sample.

CONCLUSIONS

The EPR data showed that for the dominant magnetic species there was no significant difference between the different catalysts. Further analysis of EPR spectral data showed the presence of a secondary magnetic species which is thought to be the catalytically active species. This secondary species appeared to be the more delocalized/mobile electronic species associated with surface cupric sites.

Since H^+ on the alumina surface appears necessary for the reaction, it is not surprising that the low loaded materials were better catalysts than the high loaded materials in the production of ether. The important differences shown are the chagnes in selectivity from the pure copper catalyst to the mixed $Ru–Cu/Al_2O_3$ materials, in which the selectivity is dependent on the preparation method. Here the

selectivity increases for dibutyl ether when ruthenium is present compared to when the catalyst is without ruthenium.

Another important factor is the usable lifetime of these materials. The lifetime appears to be extended by the addition of ruthenium to the Cu/Al_2O_3 materials. Ruthenium dioxide (RuO_2) seems to stabilize the catalyst allowing it to be more efficient for a significantly longer time than that seen in the pure copper material. The total percentage conversion over a 20-h time interval was much greater. This could be due to the ability of ruthenium to transfer hydrogen, allowing for the more efficient formation of the products when compared to the pure copper catalyst. It also decreases the reductive poisoning of the surface by coke formation. There is evidence of poisoning in the pure copper catalyst. Initially the fresh catalyst is a very light color compared to the used catalyst which exhibits a dark brown color. EPR analysis showed reduced signal intensity as well.

The following reaction mechanisms for these mixed metal catalysts are proposed. the primary reaction is the reduction/hydrogenation of the butyraldehyde to 1-butanol and the secondary reaction has been determined to be only the bimolecular dehydration (substitution) reaction under acidic conditions. Even though this type of system was not thought of as an acid catalyst, we have shown in this paper that it can be used as an acid catalyst in some applications. The results presented on the formation of dibutyl ether could lead to a new inexpensive process for the production of ethers.

REFERENCES

1. Crisafulli, C., Galvagno, S., Maggiore, R., Scire, S., and Saeli, A., *Catal. Lett.* **6**, 77 (1990).
2. Crisafulli, C., Maggiore, R., Schembari, G., Scire, S., and Galvagno, S., *J. Mol. Catal.* **50**, 67 (1989).
3. Galvagno, S., Crisafulli, C., Maggiore, R., Giannetto, A., and Schwank, J., *J. Therm. Anal.* **32**, 471 (1987).
4. Niwa, S., Mizukami, F., Kuno, M., Takeshita, K., Nakamura, H., Tsuchiya, T., Shimizu, K., and Imamura, J., *J. Mol. Catal.* **34**, 247 (1986).
5. Enomoto, T., Okuhara, T., and Misono, M., *Bull. Chem. Soc. Jpn.* **58**, 1490 (1985).
6. Christmann, K., Ertl, G., and Shimizu, H., *J. Catal.* **61**, 397 (1980).
7. Friedman, R. M., Freeman, J. J., and Lytle, F. W., *J. Catal.* **55**, 10 (1978).
8. Sinfelt, J. H., *Rev. Mod. Phys.* **51**, 569 (1979).
9. Voge, H. H., and Adams, C. R., *Adv. Catal.* **17**, 151 (1967).
10. Ponec, V., and Sachtler, N. M. H., *J. Catal.* **28**, 376 (1973).
11. Wade, L. G., Jr., "Organic Chemistry." Prentice Hall, New Jersey, 1995.
12. Papp, J., Soled, S., Dwight, K., and Wold, A., *Chem. Mater.* **6**, 496 (1994).
13. Voltz, S. E., Hirschler, A. E., and Smith, A., *J. Phys. Chem.* **64**, 1594 (1960).
14. British patent 718, 723 (1954).
15. Maxwell, I. E., and Naber, J. E., *Catal. Lett.* **12**, 105 (1992).
16. Biswas, J., and Maxwell, I. E., *Appl. Catal.* **58**, 1 (1990).
17. Weitkamp, J., *in* "American Chemical Society, ACS Symposium Series 20, 1975" (J. W. Ward, Ed.), p. 1–27.
18. Burgt, M. J., Leeuwen, C. J., Dell'Amico, J. J., and Sie, S. T., *in* "Methane Conversion" (D. M. Bibby, C. D. Chang, R. F. Howe, and S. Yurchak, Eds.), Elsevier Science, Amsterdam, 1988.
19. Sinfelt, J. H., *J. Catal.* **29**, 308 (1973).
20. Tanabe, K., Sumiyoshi, T., Shibata, K., Kiyoura, T., and Kitagawa, J., *Bull. Chem. Soc. Jpn.* **47**, 1064 (1974).
21. Yamaguchi, T., Tanaka, Y., and Tanabe, K., *J. Catal.* **65**, 442 (1980).
22. Shibata, K., Kiyoura, T., Kitagawa, J., Sumiyoshi, T., and Tanabe, K., *Bull. Chem. Soc. Jpn.* **46**, 2985 (1973).
23. Tanabe, K., Misono, M., Ono, Y., and Hattori, H., "New Solid Acids and Bases: Their Catalytic Properties." Elsevier Science, New York, 1989.
24. Tanabe, K., "Solid Acids and Bases." Kodansha, Tokyo, and Academic Press, New York, 1970.
25. Jobson, E., Baiker, A., and Wokaun, A., *J. Chem. Soc. Faraday Trans.* **86**(7), 1131 (1990).
26. Kung, M., and Kung, H., *Catal. Rev. Sci. Eng.* **27**, 425 (1985).
27. Peri, J., *J. Phys. Chem.* **69**, 231 (1965).
28. Asakura, C., Bando, K.-K., and Iwasawa, Y., *J. Chem. Soc. Faraday Trans.* **86**(14), 2645 (1990).
29. Black, J. B., Scott, J. D., Serwicka, E. M., and Goodenough, J. B., *J. Catal.* **106**, 16 (1987).
30. Jolly, W. L., "Modern Inorganic Chemistry." McGraw–Hill, New York, 1984.
31. Marques, E. C., Friedman, R. M., and Dahm, D., *Appl. Catal.* **19**, 387 (1985).
32. Pierron, E. D., Rashkin, J. A., and Roth, J. F., *J. Catal.* **9**, 38 (1967).
33. Matsunaga, Y., *Bull. Chem. Soc. Jpn.* **34**, 1291 (1961).
34. Berger, P. A., and Roth, J. F., *J. Phys. Chem.* **71**, 4307 (1967).
35. Fujiwara, S., Katsumata, S., and Seki, T., *J. Phys. Chem.* **71**, 115 (1967).
36. Gomez, M., "Analysis of Mixed Metal Materials as Catalysts and Electronic Ceramics," Master thesis, Temple University, Philadelphia, 1993.
37. Palmieri, M., Gomez, M. L., Vadel, N., Singh, D., and Jansen, S. A., "Materials Research Society, Symposim Proceedings, Boston, 1993," Vol. 323, p. 359. 1993.
38. Maki, A. H., and McGarvey, B. R., *J. Chem. Phys.* **29**, 31 (1958).
39. Nilges, M. J., "Electron Paramagnetic Resonance Studies of Low Symmetry Nickel(II) and Molybdenum(V) Complexes," Ph.D. thesis, University of Illinois, Urbana, 1974.
40. Kivelson, D., and Nerman, R., *J. Chem. Phys.* **35**, 149 (1961).
41. Naccache, C., and Taarit, Y. B., *Chem. Phys. Lett.* **11**, 11 (1971).
42. Niwa, M., Katsuhiro, S., Kishida, M., and Murakami, Y., *Appl. Catal.* **67**, 297–305 (1991).
43. Sinfelt, J. H., Lan, Y. L., Cusumano, J. A., and Barnett, A. E., *J. Catal.* **42**, 227 (1977).
44. McMurray, J., "Organic Chemistry." Brooks/Cole, CA, 1984.